JOURNAL OF VIROLOGY, Nov. 1997, p. 8690–8697 Vol. 71, No. 11
0022-538X/97/$04.00+0

Differential Recruitment of B and T Cells in Coxsackievirus B4-Induced Pancreatitis Is Influenced by a Capsid Protein

ARLENE I. RAMSINGH,[1,2]* WILLIAM T. LEE,[1,2] DORIS N. COLLINS,[1] AND LORI E. ARMSTRONG[1]

Wadsworth Center for Laboratories and Research, New York State Department of Health, Albany, New York 12201-2002,[1] and Department of Biomedical Sciences, School of Public Health, State University of New York at Albany, Albany, New York 12237[2]

Received 28 May 1997/Accepted 29 July 1997

Two genetically similar variants of coxsackievirus B4, CB4-P and CB4-V, cause distinct disease syndromes in mice. A multidisciplinary approach was used to examine the events occurring in situ. The CB4-P variant induced acute pancreatitis, followed by repair of the exocrine tissues, while the CB4-V variant induced chronic pancreatitis, characterized by extensive destruction of the exocrine tissues. Since CB4-V replicated more efficiently than CB4-P in vivo, the more extensive tissue injury associated with CB4-V infection could be explained as the result of a higher level of viral replication. However, the fact that CB4-V replicated more efficiently in a mouse strain that survives infection than in a strain that succumbs to infection suggests that immune-mediated mechanisms as well as viral cytolysis may contribute to pancreatic tissue injury. To address the role of the immune system in virus-induced pancreatitis, the cell types within the inflammatory infiltrate were analyzed by flow cytometry. B cells (34 to 75%) were the most abundant, followed by T cells (10 to 30%), natural killer cells (4 to 8%), and macrophages (0 to 6%). Recruitment (and perhaps proliferation) of B and T cells to the pancreatic tissues was influenced by viral strain. Differential recruitment of T and B cells may reflect altered antigenic sites between CB4-P and CB4-V. The viral sequence that affected T- and B-cell recruitment was identified as a threonine residue at position 129 of the VP1 capsid protein.

The group B coxsackieviruses, comprising six serotypes, B1–B6, are enteroviruses of the *Picornaviridae*. The viral genome consists of a single-stranded RNA of positive polarity. For coxsackievirus B4 (CVB4), the viral genome consists of 7,395 nucleotides and is composed of a 5′ untranslated region (UTR) of 743 nucleotides, a 3′ UTR of 105 nucleotides, and an open reading frame encoding a polyprotein of 2,183 amino acids which is proteolytically cleaved (12). The open reading frame is divided into three regions, P1, P2, and P3. The four capsid proteins, VP1 through VP4, are encoded within the P1 region, while the nonstructural proteins that are involved in virus replication are encoded within the P2 and P3 regions.

The group B viruses have been implicated in a variety of diseases, such as pancreatitis, type I insulin-dependent diabetes mellitus, myocarditis, and myositis (9, 16, 29). The existence of variants within a single serotype further complicates the pathogenesis of coxsackievirus infections. Although there is a great deal of information on the biochemical, biophysical, and genetic characteristics of picornaviruses, the mechanisms by which these RNA viruses cause disease are poorly understood. A powerful tool in the study of the genetic basis of virulence of picornaviruses is the use of recombinant, chimeric viruses derived from cDNA clones of virulent and avirulent viruses. Using this approach, several groups have identified determinants of attenuation or virulence for many picornaviruses. Of the three Sabin poliovirus strains, determinants of attenuation have been mapped to the 5′ UTR (13, 27, 31) and to the VP1 (15, 27, 28) and VP3 (31) coding sequences. In the mouse model, neurovirulence is determined by single amino acid substitutions in the VP1 and VP2 capsid proteins (5) and by multiple mutations in regions encoding both viral proteinase $2A^{pro}$ and the VP1 capsid protein (14). For CVB3, Zhang et al. (35) have shown that a transversion at nucleotide position 690 in the 5′ UTR is not attenuating. However, Tu et al. (30) have identified nucleotide 234 (U) in the 5′ UTR of CVB3 as a determinant of cardiovirulence. We have shown that in a mouse model of CVB4-induced pancreatitis, multiple loci in the P1 region can independently influence the virulent phenotype. In this model, thr-129 of VP1 is a major determinant of virulence (3). Arg-16 of VP4 can also influence virulence but to a lesser extent than thr-129 of VP1 (25).

In the present studies, we utilized two variants of coxsackievirus B4, CB4-V and CB4-P. Although the variants are genetically similar, they display different phenotypes both in vivo and in vitro (3, 24). In our mouse model, CB4-P (the prototypical strain JVB) causes mild pancreatitis without morbidity and is designated avirulent. The CB4-V variant is designated virulent since it induces a disease syndrome characterized by pancreatitis, hypoglycemia, and myocarditis. CB4-V infection can be lethal in mice. The outcome of infection is controlled by a locus within the major histocompatibility complex (23). In addition to viral cytolysis and autodigestion by pancreatic enzymes, immunopathological mechanisms may contribute to pancreatic tissue damage in this model. During infection with either variant, inflammatory infiltrates consisting primarily of mononuclear cells are observed in pancreatic tissues. In our continued efforts to analyze and map the phenotypic differences between the two viral variants, we addressed the following questions. (i) Which types of cells are present in the inflammatory infiltrates and what is the relative abundance of each? (ii) Is recruitment of B and T lymphocytes to the pancreas influenced by viral strain? (iii) Which viral sequences affect B- and T-cell recruitment to the pancreas?

* Corresponding author. Mailing address: Wadsworth Center for Laboratories and Research, New York State Department of Health, 120 Scotland Ave., Albany, NY 12201-2002. Phone: (518) 474-8634. Fax: (518) 474-3181. E-mail: arlene.ramsingh@wadsworth.org.

MATERIALS AND METHODS

Cells and viruses. The passage histories of the two viruses, CB4-P and CB4-V, have been previously described (23). After plaque purification, large scale stocks

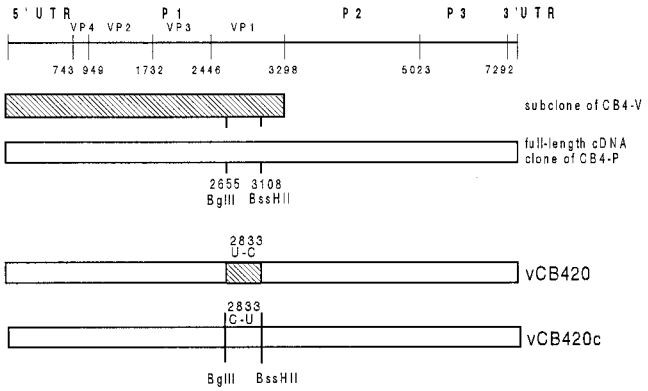

FIG. 1. Genotypes of recombinant chimeric coxsackieviruses. The top line depicts the structural organization of the coxsackievirus B4 (strain JVB) genome (12). The vCB420 recombinant was constructed from a subclone of CB4-V and a full-length clone of CB4-P. The vCB420c control virus was constructed by replacing the *Bgl*II-*Bss*HII fragment of the full-length cDNA of vCB420 with the corresponding fragment from the cDNA clone of CB4-P.

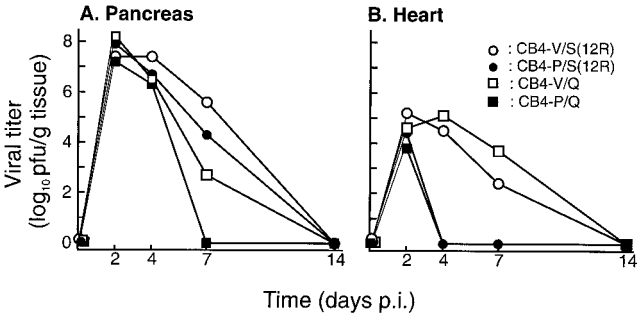

FIG. 2. Replication of CB4-P and CB4-V in pancreatic and cardiac tissues of mice. Two B10 H-2 congenic strains of mice, B10.S(12R) and B10.Q, were infected intraperitoneally with either variant. Pancreatic and cardiac tissues were harvested at different times p.i. Homogenates of pooled tissues were assayed for viral infectivity. (A and B) Viral replication in pancreatic (A) and cardiac (B) tissues. These experiments were performed three times each, and representative results are shown.

of CB4-P and CB4-V were prepared in HeLa cells and LLC-MK2(D) cells, respectively. Viral infectivity was determined by plaque assay with LLC-MK2(D) cells. Construction of the recombinant virus, vCB420, has been previously reported (3). Briefly, a *Bgl*II-*Bss*HII fragment from a subclone of CB4-V, containing a single point mutation at nucleotide position 2833, was used to replace the corresponding fragment in a full-length cDNA clone of CB4-P (Fig. 1). The resulting virus, vCB420, contains a threonine residue at position 129 of VP1 on the avirulent CB4-P genetic background. A control virus, designated vCB420c, was reconstructed from vCB420 to replace threonine at position 129 of VP1 with a methionine residue, thereby regenerating the parental CB4-P virus. The strategy used for constructing vCB420c was similar to the one used for constructing vCB420. The *Bgl*II-*Bss*HII fragment of the full-length cDNA of vCB420 was replaced with the corresponding fragment from the cDNA clone of CB4-P. Recombinant virus was obtained by transfecting LLC-MK2(D) cells with in vitro-derived RNA transcripts. Virus was harvested when cells exhibited 80 to 100% cytopathic effect and were subsequently plaque purified. Limited sequence analysis of the viral genomic RNA confirmed the nucleotide substitution at position 2833. The resulting recombinant virus should recapitulate the phenotype of CB4-P. The vCB420c construct controls for mutations that may have occurred outside the *Bgl*II-*Bss*HII region that might influence the phenotype of vCB420. Infection of B10.T(6R) mice resulted in 0% morbidity in CB4-P-infected mice and 100% morbidity in vCB420-infected mice (3). Like CB4-P-infected mice, B10.T(6R) mice survived infection with vCB420c. This result suggests that if substitutions occurred outside the *Bgl*II-*Bss*HII region during the construction of vCB420, they did not affect the virulent phenotype.

Infection of mice. Three B10 *H-2* congenic strains of mice, B10.T(6R), B10.Q, and B10.S(12R), were used in these studies. These strains were bred in our animal facility. Four- to six-week-old mice were injected intraperitoneally with 10^4 PFU of virus diluted in phosphate-buffered saline. Control mice were injected with phosphate-buffered saline. All injected mice were monitored daily. Animals found to be moribund were euthanized immediately by CO_2 overdose. All animal procedures were approved by the Institutional Animal Care and Use Committee of the Wadsworth Center. Mice were sacrificed at various times postinfection (p.i.), and organs (pancreas, heart, and spleen) were harvested. Tissue homogenates were prepared as previously described (23) and assayed for infectivity by plaque assay. Pancreatic tissues fixed in phosphate-buffered formalin were processed for routine histology, followed by staining with hematoxylin and eosin.

Flow cytometry. Previous studies have shown that of the B10 *H-2* congenic strains tested, B10.T(6R) mice are most sensitive to infection with CB4-V, while B10.S(12R) mice are most resistant (23). Pancreatic inflammatory infiltrates and spleen cells from both strains were analyzed by flow cytometry (4). Surface markers examined included CD4, CD8, CD45R/B220, NK1.1, and MAC-1 (CD11b). Mice were infected intraperitoneally with either CB4-P or CB4-V. Pancreata and spleens were harvested at days 5 and 7 p.i. Spleen cell suspensions were obtained by mechanical disruption (4). We reasoned that a similar approach would release the infiltrating cells from the pancreas. Mononuclear cells were isolated by Ficoll-Paque gradient centrifugation (4). After being washed in Dulbecco modified Eagle medium, viable cells were counted and stained directly with fluorescein isothiocyanate (FITC)- and R-phycoerythrin (R-PE)-conjugated rat anti-mouse monoclonal antibodies (PharMingen) for two-color analysis by the Becton Dickinson FACScan. To obtain sufficient numbers of cells for flow cytometric analysis, the infiltrates from two to three pancreata were pooled. A minimum of 10^5 infiltrating cells was used for two-color analysis. The number of cells isolated from a single spleen ranged from 3×10^7 to 6×10^7, and samples of 10^6 cells were processed for staining.

RESULTS

Viral replication in vivo. To study viral replication in vivo, the presence of infectious virus in tissue homogenates was examined by plaque assay. Infectivity assays were carried out on pooled tissue samples (3 to 5 tissues per group) and individual tissue samples at various times after infection. Experiments were performed three times each. No significant difference was observed between titers from pooled tissue samples and those from individual tissues. Representative results from infectivity assays of pooled tissue samples are shown in Fig. 2. Of the *H-2* congenic strains, B10.T(6R) is the most susceptible to CB4-V infection and succumbs at 7 to 14 days p.i. These studies were therefore confined to B10.Q and B10.S(12R) mice, which, when infected with CB4-V, exhibit morbidity rates of 43 to 69 and 0%, respectively (23). Viral titers for both CB4-P and CB4-V peaked at day 2 p.i. in pancreatic tissues. CB4-V replicated to higher titers than CB4-P. This difference was most obvious at day 7 p.i., when titers of CB4-V were 20-fold [B10.S(12R)] and 500-fold [B10.Q] greater than those of CB4-P. Both CB4-P and CB4-V grew to higher titers in B10.S(12R) than in B10.Q mice. Infectious CB4-V was cleared by 2 weeks p.i. Infectious CB4-P was cleared between 1 and 2 weeks p.i.

Since the group B coxsackieviruses can also replicate in cardiac tissues, the presence of infectious virus in heart homogenates was examined by plaque assay (Fig. 2B). CB4-V replicated in cardiac tissues of both B10.S(12R) and B10.Q mice but to lower levels than in pancreatic tissues. Cardiac tissues did not support replication of CB4-P, since infectious virus was not detected after 2 days of infection. The viral titer observed at day 2 p.i. is coincident with viremia, which also peaks at day 2 p.i. (data not shown).

Coxsackievirus B4-induced pancreatitis. Previous histological studies (3) have been focused on the early events in infection (day 2 p.i.). To examine the extent of tissue destruction, a histological study of pancreatic tissues harvested at various times p.i. (1 to 14 days) from B10.S(12R) and B10.Q mice infected with either CB4-P or CB4-V was undertaken. Morphological alterations in both strains of mice were similar. A composite of representative results from infected B10.S(12R) mice is shown in Fig. 3 and 4. Acute infection, reflected by increasing viral titers, is depicted in Fig. 3. Post-acute infection,

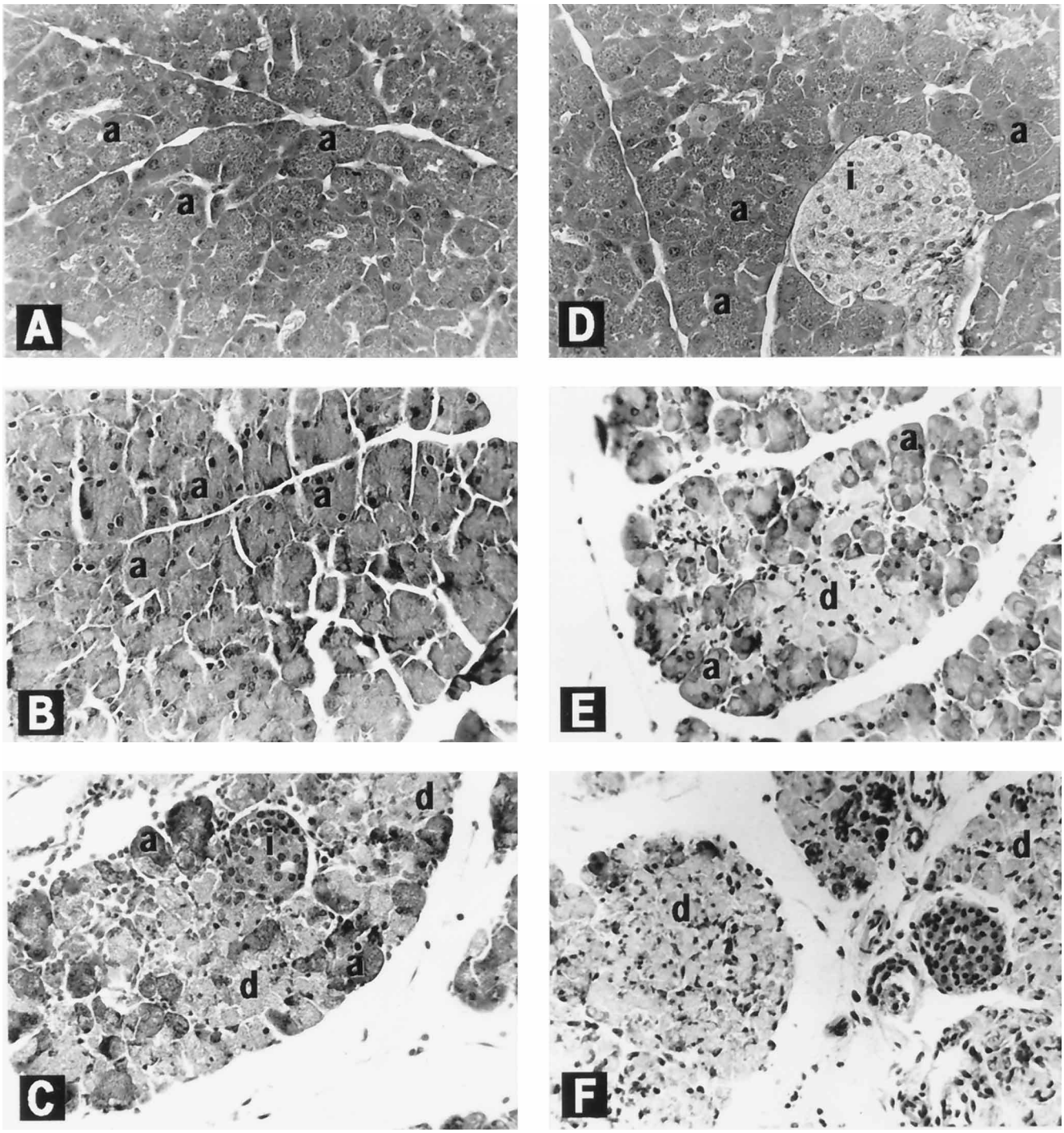

FIG. 3. Histopathology of pancreatic tissues from CB4-P- and CB4-V-infected B10.S(12R) mice during acute stage of infection. Mice were infected intraperitoneally with either variant, and pancreatic tissues were harvested at various times p.i., processed for histology, and stained with hematoxylin and eosin. (A and D) mock-infected; (B) CB4-P, day 1 p.i.; (C) CB4-P, day 2 p.i.; (E) CB4-V, day 1 p.i.; (F) CB4-V, day 2 p.i. a, acinus; i, islet of Langerhans; d, degranulated acinar cells. Magnification, ×185.

reflected by diminishing viral titers, is depicted in Fig. 4. Both viral variants affect the exocrine pancreas, while the endocrine pancreas, the islets of Langerhans, appear unaffected at the light microscopic level. The structural unit of the exocrine pancreas is the acinus, which consists of a group of acinar cells surrounding a central lumen. The acinar cells produce digestive enzymes which are packaged into zymogen granules, released into pancreatic ducts, and eventually transported to the duodenum.

Infection of mice with CB4-P resulted in acute pancreatitis, followed by tissue repair 2 weeks later. During the first 2 days of infection, the acinar cells of the exocrine pancreas had a shrunken appearance (Fig. 3B and C). By day 2 p.i., foci of degranulated acinar cells were evident (Fig. 3C). By day 4 p.i.,

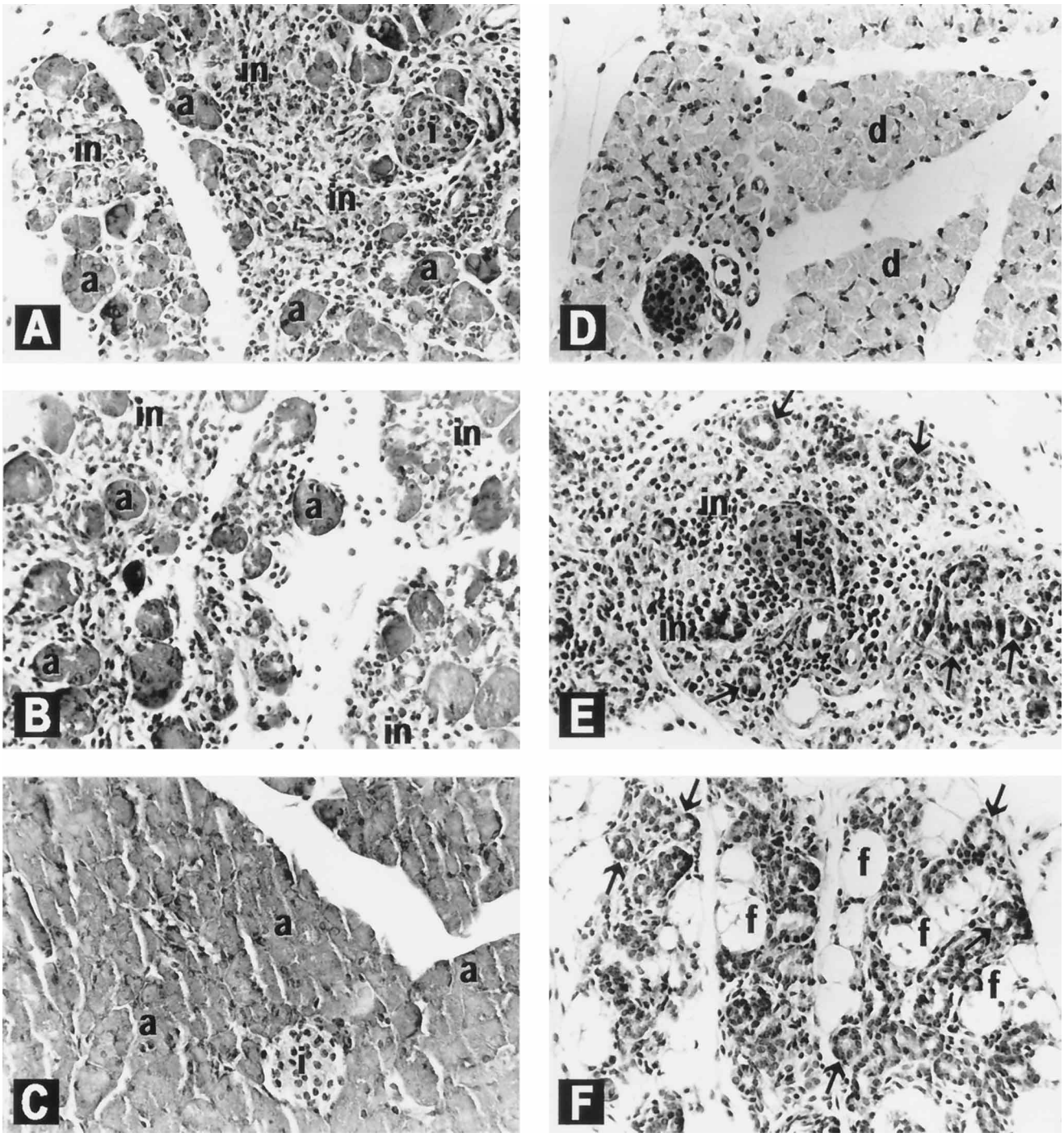

FIG. 4. Histopathology of pancreatic tissues from CB4-P- and CB4-V-infected B10.S(12R) mice during the postacute stage of infection. Mice were infected intraperitoneally with either variant, and pancreatic tissues were harvested at various times p.i., processed for histology, and stained with hematoxylin and eosin. (A) CB4-P, day 4 p.i.; (B) CB4-P, day 7 p.i.; (C) CB4-P, day 14 p.i.; (D) CB4-V, day 4 p.i.; (E) CB4-V, day 7 p.i.; (F) CB4-V, day 14 p.i. a, acinus; i, islet of Langerhans; d, degranulated acinar cells; in, inflammatory infiltrate; f, fat-cell necrosis. Arrows show tubular/ductular structures. Magnification, ×185.

approximately 5% of the acini were lost (Fig. 4A). The remaining cells showed some depletion in zymogen granules. From day 4 to day 7 p.i., an inflammatory infiltrate consisting primarily of mononuclear cells was observed. By day 7, although pancreatic architecture was disrupted, foci of degranulated acini were evident (Fig. 4B). Virus was cleared by day 14 p.i. (Fig. 2A), at which time the exocrine pancreas had healed (Fig. 4C). Pancreatic architecture was restored, and inflammatory infiltrates were no longer evident.

Mice infected with CB4-V developed chronic pancreatitis with extensive damage to the exocrine pancreas. During the first 2 days of infection, there was extensive degranulation of the acinar cells (Fig. 3E and F). By day 4, extensive acinar cell necrosis involving approximately 98% of acinar cells was ob-

served Fig. 4D). The remaining acini had fewer zymogen granules. As in CB4-P-infected mice, an inflammatory infiltrate consisting primarily of mononuclear cells was observed from day 4 to day 7 p.i. Unlike in CB4-P-infected mice, acini were no longer evident by day 7 p.i. (Fig. 4E). Numerous ductular structures suggestive of acinoductular metaplasia were apparent. The presence of tubular/ductular complexes, also referred to as pseudoductules (26), in a variety of pancreatic diseases, including pancreatitis, cystic fibrosis, and pancreatic cancers, is well documented (19–21, 33). The presence of these ductular complexes may reflect the extent of acinar injuries (26). Extensive tissue injury, associated with CB4-V infection, correlated with numerous ductular structures, while lesser injury observed with CB4-P infection correlated with very few ductular structures. In CB4-V infected mice, by day 14 p.i., tubular structures, but no acini, were observed (Fig. 4F). Replacement of the destroyed acini with fat cells resulted in fat-cell necrosis. Mild inflammation was evident.

In summary, CB4-V infection resulted in chronic pancreatitis, characterized by extensive necrosis of the acinar cells, while CB4-P infection resulted in acute pancreatitis, followed by tissue repair. A comparable histological study of B10.Q mice infected with either CB4-P or CB4-V yielded similar results (data not shown).

Phenotyping of pancreatic inflammatory infiltrates by flow cytometry. During infection with either CB4-P or CB4-V, an inflammatory infiltrate consisting primarily of mononuclear cells is observed in pancreatic tissues from days 4 to 7 p.i. (Fig. 3 and 4). The inflammatory infiltrate was analyzed by flow cytometry to identify the cell types within the infiltrate and to determine the relative abundance of each cell type. Spleen cells were processed in parallel as controls. Surface markers analyzed included CD4 ($CD4^+$ T cells), CD8 ($CD8^+$ T cells), CD45R/B220 (B cells and activated T cells), NK1.1 (natural killer cells), and MAC-1 (CD11b) (macrophages and natural killer cells). Although the B220 marker can also be present on activated T cells, two-color analysis with anti-B220 and either anti-CD4 or anti-CD8 did not detect doubly stained ($B220^+$, $CD4^+$ or $B220^+$, $CD8^+$) subsets of cells. Two-color analysis with anti-B220 and anti-NK1.1 resulted in the detection of a transient, doubly labeled natural killer cell subset in CB4-V-infected cells (see below). However, the level of B220 expression in this subset was low, allowing us to differentiate between the natural killer and B-cell populations.

Histological analyses revealed that the inflammatory infiltrate consisted primarily of mononuclear cells. To ensure that our handling of the infiltrates and the spleen cell suspensions did not result in the loss of specific subsets of mononuclear cells, spleen cells from uninfected mice were purified by Ficoll-Paque gradient centrifugation and stained with the panel of monoclonal antibodies to detect $CD4^+$ T cells, $CD8^+$ T cells, macrophages, natural killer cells, and B cells (three times for each mouse strain). Recovery of mononuclear cells ranged from 90 to 96%.

Both B10.T(6R) and B10.S(12R) mice were studied, since CB4-V infection of these two strains results in 100 and 0% morbidity, respectively (23). Infected mice were sacrificed, and the cellular infiltrates from pancreatic tissues were harvested at 5 and 7 days p.i. and processed for staining with labeled anti-mouse monoclonal antibodies for two-color analysis by flow cytometry. Spleen cells were processed in parallel. Each experiment was performed three to seven times. Representative results from the two-color analysis are shown in Fig. 5. Summarized data are shown in Fig. 6 and Table 1. The pancreatic inflammatory infiltrate consisted of B cells, $CD4^+$ T cells, $CD8^+$ T cells, macrophages, and natural killer cells. T and B cells predominated in the infiltrate. Recruitment of B cells and $CD4^+$ T cells to the pancreas was affected by viral strain. A higher percentage of B cells was observed in the inflammatory infiltrates from CB4-P-infected mice at both days 5 and 7 p.i., regardless of the mouse strain infected (Fig. 6A). A higher percentage of $CD4^+$ T cells was observed in the pancreatic infiltrates from CB4-V-infected mice (Fig. 6C). This difference was most pronounced at day 5 p.i. Differential recruitment of B and T cells was also observed in infected B10.Q mice (data not shown).

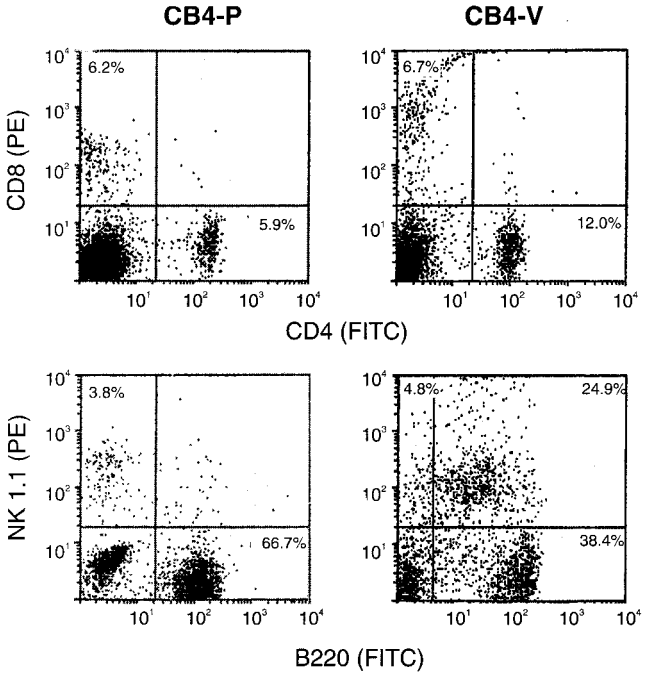

FIG. 5. Two-color flow cytometric analyses of pancreatic inflammatory infiltrates from CB4-P- and CB4-V-infected mice. Inflammatory cells were purified from pancreatic tissues that were harvested at 5 days p.i. from B10.S(12R) mice. Cells were stained with antimouse monoclonal antibodies for two-color analysis. Upper two panels, representative results of staining with R-PE-labeled anti-CD8 and FITC-labeled anti-CD4; bottom two panels, representative results of staining with R-PE-labeled anti-NK1.1 and FITC-labeled anti-B220.

Since the differential recruitment of B and T cells to the pancreas during infection is dependent on viral strain, in subsequent studies we mapped the viral locus that influenced this phenotype. In previous studies with a panel of recombinant, chimeric viruses, a major determinant of virulence at VP1-129 was identified (3). The recombinant virus, vCB420, which contains a threonine residue at position 129 of VP1 on the avirulent (CB4-P) genetic background, was used to infect B10.T(6R) mice. Analysis of the inflammatory infiltrate at day 5 p.i. revealed a low percentage of B cells and a high percentage of $CD4^+$ T cells (Fig. 6A and C), the phenotype that is observed in CB4-V-infected mice. $CD4^+$ T cells comprised an even higher percentage of the infiltrate in vCB420-infected mice than they did in CB4-V-infected mice. To control for the presence of additional sites that may influence this phenotype, an additional chimeric virus, vCB420c, was reconstructed from vCB420 to replace threonine at position 129 of VP1 with a methionine residue, thereby regenerating the parental CB4-P virus. The composition of the inflammatory infiltrate from mice infected with vCB420c was similar to that from CB4-P-infected mice (66 to 70% B cells and 4 to 6% $CD4^+$ T cells). Viral infection did not alter the percentage of B cells within the

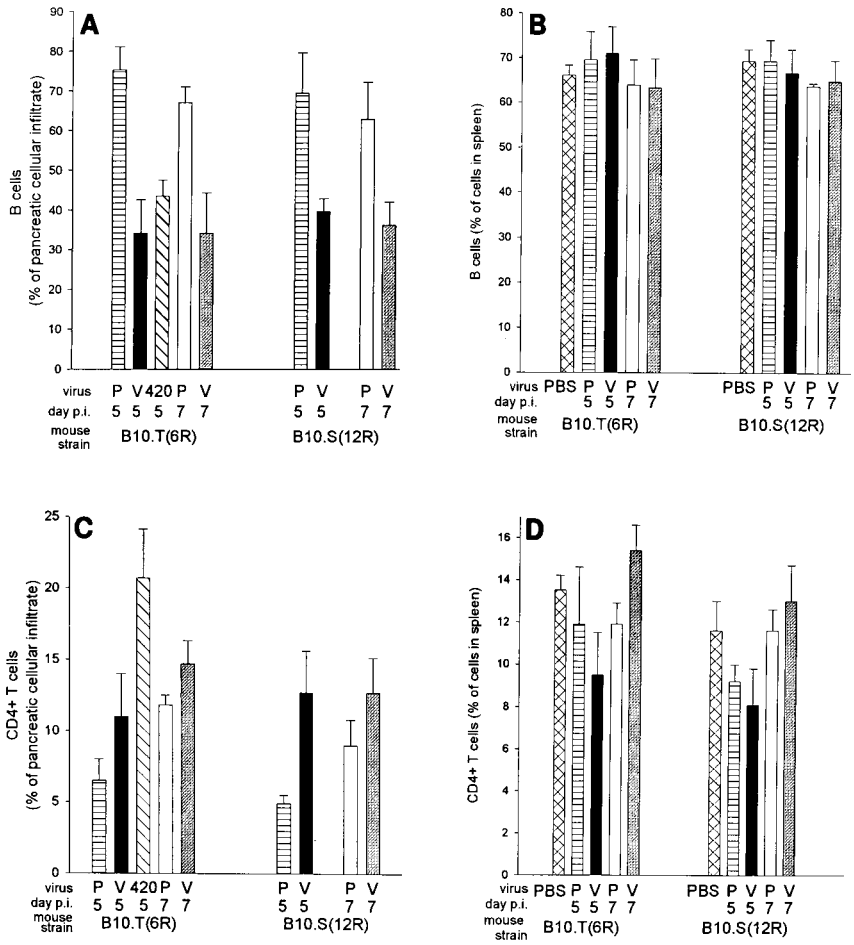

FIG. 6. Summary of flow cytometric analyses of $CD4^+$ T cells and B cells in the inflammatory infiltrates of CVB4-infected mice. Inflammatory cells were purified from pancreatic tissues of B10.T(6R) and B10.S(12R) mice that had been infected with CB4-P (P), CB4-V (V), or vCB420 (420). Cells were stained with anti-B220 and anti-CD4. Spleen cells were processed in parallel. Experiments were performed 3 to 7 times each. Mean values (and standard deviations) are shown. PBS, phosphate-buffered saline.

spleen (Fig. 6B). Infection with CB4-V resulted in a decrease in splenic $CD4^+$ T cells at day 5 p.i. in both strains of mice (Fig. 6D). By day 7, the $CD4^+$ T cell population had reached normal values. The significance of this decrease is not understood.

In analyzing the natural killer cell populations, we observed two subsets of cells in infected mice (Table 1). One subset of cells expressed the NK1.1 marker and comprised 4.0 to 7.6% of the inflammatory infiltrate. The second subset of natural killer cells expressed the NK1.1 marker and low levels of the CD45R/B220 marker. The $NK1.1^+$, $CD45R/B220^+$ subset was a transient population that was present in CB4-V-infected mice at 5 days p.i. By day 7 p.i., this subset was no longer detected. The doubly stained natural killer cells were not observed in CB4-P-infected mice. Lymphokine-activated killer cells can be divided into two subsets, $NK1.1^+$, $CD8^-$ (natural killer cells) and NK1.1-$CD8^+$ (T cells) (1). The lytically active subset of each group also expresses B220 (1). The $NK1.1^+$, $CD45R/B220^+$ subset in our model may represent lymphokine-activated natural killer cells, but additional characterization will be necessary to clarify the identity of this subpopulation. In infected mice, 3.1 to 13.1% of the infiltrate stained with anti-MAC-1, which detects macrophages and natural killer cells. Since $NK1.1^+$ cells account for 4 to 7.6% of the cells, the percentage of macrophages in the infiltrate is low (0 to 5.5%). Viral infection did not significantly alter the percentages of $CD8^+$ T cells, macrophages, or natural killer cells in the spleens of infected mice.

DISCUSSION

In our model, two genetically similar variants of coxsackievirus B4, CB4-P and CB4-V, caused distinct disease syndromes in mice. The CB4-P variant induced acute pancreatitis, followed by repair of the exocrine tissues. The CB4-V variant induced chronic pancreatitis, characterized by extensive destruction of the exocrine tissues. Tissue repair was not observed in the 2-week follow-up study. Chronic versus acute pancreatitis is a phenotype that is dependent on the infecting viral strain, not on mouse strain. The main difference between acute and chronic pancreatitis is that the morphologic alterations seen in acute pancreatitis are entirely reversible, with the pancreatic architecture returning to normal in a relatively short period of time, while the changes observed in chronic pancreatitis are irreversible (6, 7, 11).

To determine if the two viruses had different growth properties in vivo, pancreatic homogenates were assayed for infectivity at different times p.i. The CB4-V variant replicated more efficiently than the CB4-P variant. This result suggests that in

TABLE 1. Summary of flow cytometric analyses of $CD8^+$ T cells, macrophages, and natural killer cells in the inflammatory infiltrates of CVB4-infected mice[a]

Mouse strain	Virus or PBS[c]	Tissue	Days p.i.	% of cells stained [mean (SD)]			
				Anti-CD8	Anti-MAC-1	Anti-NK1.1	Anti-NK1.1 and anti-B220
B10.T(6R)	PBS	Spleen		7.3 (1.1)	5.6 (0.6)	1.9 (0.1)	
	CB4-P	Spleen	5	6.8 (1.6)	7.6 (0.7)	0.8 (0.7)	
	CB4-V	Spleen	5	8.4 (1.3)	6.1 (0.6)	1.5 (0.9)	
	CB4-P	Spleen	7	6.2 (0.6)	4.1 (0.7)	2.2 (0.6)	
	CB4-V	Spleen	7	7.2 (1.0)	6.8 (1.4)	2.8 (1.5)	
	CB4-P	Pancreas	5	7.1 (2.8)	6.6 (0.7)	5.1 (3.9)	
	CB4-V	Pancreas	5	8.1 (1.8)	7.7 (1.9)	6.6 (1.0)	19.4 (1.5)
	CB4-P	Pancreas	7	7.4 (5.0)	3.1 (0.4)	4.9 (3.0)	
	CB4-V	Pancreas	7	7.8 (1.0)	ND[b]	4.0 (2.1)	
B10.S(12R)	PBS	Spleen		6.3 (2.5)	8.5 (0.2)	0.8 (1.1)	
	CB4-P	Spleen	5	6.1 (0.1)	7.7 (1.0)	1.2 (0.8)	
	CB4-V	Spleen	5	9.2 (0.1)	8.5 (1.2)	1.1 (0.8)	
	CB4-P	Spleen	7	7.0 (0.7)	5.8 (0.2)	1.7 (0.8)	
	CB4-V	Spleen	7	9.9 (2.3)	1.1 (0.7)	2.0 (0)	
	CB4-P	Pancreas	5	4.7 (0.5)	13.1 (2.4)	7.6 (4.5)	
	CB4-V	Pancreas	5	6.1 (0.8)	6.1 (1.4)	4.0 (1.6)	20.1 (6.2)
	CB4-P	Pancreas	7	6.7 (1.7)	7.1 (1.8)	6.4 (2.8)	
	CB4-V	Pancreas	7	10.8 (3.2)	3.8 (1.8)	4.1 (2.0)	

[a] Inflammatory cells were purified from pancreatic tissues of B10.T(6R) and B10.S(12R) mice that had been infected with CB4-P or CB4-V. Cells were stained with the appropriate monoclonal antibodies. Spleen cells were processed in parallel. Experiments were performed 3 to 7 times each.
[b] ND, not done.
[c] PBS, phosphate-buffered saline.

CB4-V-infected mice, a higher level of viral replication results in extensive destruction of the exocrine tissues, precluding a regenerative response. This supports the idea that the magnitude of the regenerative response is dependent on the extent of acinar cell necrosis (26). In CB4-P-infected mice, a lower level of viral replication results in less tissue injury and is compatible with tissue repair. Since the outcome of infection with CB4-V is influenced by the major histocompatibility complex haplotype (23), viral replication in two *H-2* congenic strains [B10.S(12R) and B10.Q] was analyzed. CB4-V infection of these two strains results in more extensive tissue injury in B10.Q mice, with morbidity rates of 43 to 69%. CB4-V infection is not lethal in B10.S(12R) mice. Surprisingly, CB4-V grew to higher titers in B10.S(12R) mice. If pancreatic tissue destruction was due solely to viral cytolysis, then CB4-V would be expected to replicate to higher titers in B10.Q mice. Instead, CB4-V replicated to higher titers in B10.S(12R) mice, suggesting that tissue damage in CB4-V-infected mice may be due to immune-mediated mechanisms in addition to viral cytolysis. Studies of myocardial damage during CVB3 infection have yielded conflicting data. Whether tissue damage is due solely to the virus, to immunopathological mechanisms, or to a combination of both is unclear. Evidence supporting an immunopathological mechanism implicates different effector cells, such as cytotoxic T cells (10), $CD4^+$ T cells (2, 10), autoantibody-producing B cells (18, 34), and natural killer cells (8). To address the role of the immune system in pancreatic tissue damage during CB4-V infection, a study of the inflammatory infiltrate was undertaken. Histological studies showed that infection with either virus resulted in infiltrates consisting primarily of mononuclear cells. To identify the types of cells present within the infiltrate and the relative abundance of each cell type, the inflammatory cells were analyzed by flow cytometry. B cells (34 to 75%) were the most abundant, followed by T cells (10 to 30%), natural killer cells (4 to 8%), and macrophages (0 to 6%). A transient population of natural killer cells expressing the NK1.1 and CD45R/B220 markers was observed in CB4-V-infected mice at day 5 p.i. and accounted for 19 to 20% of the infiltrate. Recruitment (and perhaps proliferation) of B and T cells to the pancreatic tissues was influenced by viral strain. Comparison of the infiltrates from infected mice showed that the inflammatory cells from CB4-P-infected mice contained a higher percentage of B cells and a lower percentage of $CD4^+$ T cells. Differential recruitment of T and B cells during viral-induced pancreatitis may reflect altered antigenic sites between CB4-P and CB4-V. The viral sequence that affected T- and B-cell recruitment was identified as a threonine residue at position 129 of the VP1 capsid protein, a site that has been shown to be a major determinant of virulence (3). Threonine-129 is predicted to lie within the DE loop of VP1 (17, 22). The DE loop of VP1 of poliovirus affects antigenicity and host range (27, 32). To assess the role of the DE loop of VP1 of coxsackievirus B4 in pathogenesis, we are examining both antigenicity and tropism, with an emphasis on the effect of substituting a threonine residue at position 129.

The approach used to analyze the infiltrating cells in the pancreas allowed a gross evaluation of inflammation in situ. Since CB4-V infection results in 100% morbidity in B10.T(6R) mice and 0% morbidity in B10.S(12R) mice (23), the pancreatic inflammatory infiltrates of both strains were analyzed and compared. Subtle differences between the two strains would not be detected in this type of analysis. The only significant difference observed was a temporal one, in that more $CD8^+$ T cells were present in the pancreatic infiltrates of infected B10.S(12R) mice at day 7 than at day 5 p.i. (Table 1). This difference was more apparent in comparisons of ratios of B/T cells and $CD4^+/CD8^+$ T cells (Table 2). In B10.T(6R) mice, the percent of $CD8^+$ T cells remained the same at the two different time points, resulting in similar ratios of B/T cells and $CD4^+/CD8^+$ T cells. Higher numbers of $CD8^+$ T cells in infected B10.S(12R) mice may reflect increased recruitment or proliferation. Since B10.S(12R) mice survive infection with

TABLE 2. Ratios of B- and T-cell subsets in the pancreatic inflammatory infiltrates of CB4-V-infected mice

Cell ratio	Days p.i.	Ratio of cell subsets[a] in mouse strain:	
		B10.T(6R)	B10.S(12R)
B/T cells	5	1.8	2.6
	7	1.9	1.6
B/CD8$^+$ T cells	5	4.2	7.9
	7	5.5	3.8
B/CD4$^+$ T cells	5	3.1	3.8
	7	2.9	2.6
CD4$^+$/CD8$^+$ T cells	5	1.4	2.1
	7	1.9	1.2

[a] Ratios were determined with mean values obtained from three to seven experiments.

CB4-V, the increased recruitment and/or proliferation of CD8$^+$ T cells later in infection may reflect a protective function (perhaps by suppressor T cells). The role of CD8$^+$ T cells in the pathogenesis of CVB4-induced pancreatitis is being examined in ongoing studies.

ACKNOWLEDGMENTS

This work was supported by Public Health Service grant DK43929 (A.R.) from the National Institute of Diabetes and Digestive and Kidney Diseases and by the American Heart Association (W.T.L.).

The facilities and services of the Cellular Immunology Core Facility and the Molecular Genetics Core Facility were used for this study. The technical expertise of Bob Dilwith in flow cytometry was greatly appreciated. We thank the staff of the Department of Pathology at the Wadsworth Center for processing tissue samples for histology.

REFERENCES

1. **Ballas, Z. K., and W. Rasmussen.** 1990. Lymphokine-activated killer (LAK) cells. IV. Characterization of murine LAK effector subpopulations. J. Immunol. **144:**386–395.
2. **Blay, R., K. Simpson, K. Leslie, and S. A. Huber.** 1989. Coxsackievirus-induced disease: CD4$^+$ cells initiate both myocarditis and pancreatitis in DBA/2 mice. Am. J. Pathol. **135:**899–907.
3. **Caggana, M., P. Chan, and A. Ramsingh.** 1993. Identification of a single amino acid residue in the capsid protein VP1 of coxsackievirus B4 that determines the virulent phenotype. J. Virol. **67:**4797–4803.
4. **Coligan, J. E., A. M. Kruisbeek, D. H. Margulies, E. M. Shevach, and W. Strober.** 1996. Current protocols in immunology. John Wiley & Sons, New York, N.Y.
5. **Couderc, T., J. Hogle, H. Le Blay, F. Horaud, and B. Blondel.** 1993. Molecular characterization of mouse-virulent poliovirus type 1 Mahoney mutants: involvement of residues of polypeptides VP1 and VP2 located on the inner surface of the capsid protein shell. J. Virol. **67:**3808–3817.
6. **DiMagno, E. P., and J. E. Clain.** 1986. Chronic pancreatitis, p. 541–575. *In* V. L. W. Go, J. D. Gardner, F. P. Brooks, E. Lebenthal, E. P. DiMagno, and G. A. Scheele (ed.), The exocrine pancreas: biology, pathobiology, and diseases. Raven Press, New York, N.Y.
7. **Elsasser, H. P., G. Adler, and H. F. Kern.** 1986. Time course and cellular source of pancreatic regeneration following acute pancreatitis in the rat. Pancreas **1:**421–429.
8. **Godeny, E. K., and C. J. Gauntt.** 1987. Murine natural killer cells limit coxsackievirus B3 replication. J. Immunol. **139:**913–918.
9. **Grist, N. R., E. J. Bell, and F. Assaad.** 1978. Enteroviruses in human disease. Prog. Med. Virol. **24:**114–157.
10. **Henke, A., S. Huber, A. Stelzner, and J. L. Whitton.** 1995. The role of CD8$^+$ T lymphocytes in coxsackievirus B3-induced myocarditis. J. Virol. **69:**6720–6728.
11. **Iovanna, J. L., C. Odaira, Z. Berger, and H. Sarles.** 1988. Temporary pseudochronic lesions during the recovery of acute necrohemorrhagic pancreatitis in rabbits. Pancreas **3:**433–438.
12. **Jenkins, O., J. Booth, P. Minor, and J. Almond.** 1987. The complete nucleotide sequence of coxsackievirus B4 and its comparison to other members of the Picornaviridae. J. Gen. Virol. **68:**1835–1848.
13. **Kawamura, N., M. Kohara, S. Abe, T. Komatsu, K. Tago, M. Arita, and A. Nomoto.** 1989. Determinants in the 5′ noncoding region of poliovirus Sabin 1 RNA that influence the attenuation phenotype. J. Virol. **63:**1302–1309.
14. **Lu, H.-H., C. F. Yang, A. D. Murdin, M. H. Klein, J. J. Harber, O. M. Kew, and E. Wimmer.** 1994. Mouse neurovirulence determinants of poliovirus type 1 strain LS-a map to the coding regions of capsid protein VP1 and proteinase 2A^{pro}. J. Virol. **68:**7507–7515.
15. **Macadam, A. J., S. R. Pollard, G. Ferguson, G. Dunn, R. Skuce, J. W. Almond, and P. D. Minor.** 1991. The 5′ noncoding region of the type 2 poliovirus vaccine strain contains determinants of attenuation and temperature sensitivity. Virology **181:**451–458.
16. **Melnick, J. L.** 1985. Enteroviruses: polioviruses, coxsackieviruses, echoviruses, and newer enteroviruses, p. 739–794. *In* B. N. Fields, D. M. Knipe, R. M. Chanock, J. L. Melnick, B. Roizman, and R. E. Shope (ed.), Virology. Raven Press, New York, N.Y.
17. **Muckelbauer, J. K., M. Kremer, I. Minor, G. Diana, F. J. Dutko, J. Groarke, D. C. Pevear, and M. G. Rossmann.** 1995. The structure of coxsackievirus B3 at 3.5 A resolution. Structure **3:**653–667.
18. **Neu, N., K. W. Beisel, M. D. Traystman, N. R. Rose, and S. W. Craig.** 1987. Autoantibodies specific for the cardiac myosin isoform are found in mice susceptible to coxsackievirus B3-induced myocarditis. J. Immunol. **138:**2488–2492.
19. **Noronha, M., O. R. Bordalo, and D. A. Dreiling.** 1981. Alcohol and the pancreas II. Pancreatic morphology of advanced alcoholic pancreatitis. J. Gastroenterol. **76:**120–124.
20. **Parsa, I., D. S. Longnecker, D. G. Scarpelli, P. Pour, J. K. Reddy, and M. Lefkowitz.** 1985. Ductal metaplasia of human exocrine pancreas and its association with carcinoma. Cancer Res. **45:**1285–1290.
21. **Porta, E. A., A. A. Stein, and P. Patterson.** 1964. Ultrastructural changes of the pancreas and liver in cystic fibrosis. Am. J. Clin. Pathol. **42:**451–465.
22. **Ramsingh, A., H. Araki, S. Bryant, and A. Hixson.** 1992. Identification of candidate sequences that determine virulence in coxsackievirus B4. Virus Res. **23:**281–292.
23. **Ramsingh, A., J. Slack, J. Silkworth, and A. Hixson.** 1989. Severity of disease induced by a pancreatropic coxsackie B4 virus correlates with the H-2K^q locus of the major histocompatibility complex. Virus Res. **14:**347–358.
24. **Ramsingh, A. I., M. Caggana, and S. Ronstrom.** 1995. Genetic mapping of the determinants of plaque morphology of coxsackievirus B4. Arch. Virol. **140:**2215–2226.
25. **Ramsingh, A. I., and D. N. Collins.** 1995. A point mutation in the VP4 coding sequence of coxsackievirus B4 influences virulence. J. Virol. **69:**7278–7281.
26. **Rao, M. S., A. V. Yeldandi, and J. K. Reddy.** 1990. Differentiation and cell proliferation patterns in rat exocrine pancreas: role of type I and type II injury. Pathobiology **58:**37–43.
27. **Ren, R., E. G. Moss, and V. R. Racaniello.** 1991. Identification of two determinants that attenuate vaccine-related type 2 poliovirus. J. Virol. **65:** 1377–1382.
28. **Tatem, J. M., C. Weeks-Levy, A. Georgiu, S. J. DiMichele, E. J. Gorgacz, V. R. Racaniello, F. R. Cano, and S. J. Mento.** 1992. A mutation present in the amino terminus of Sabin 3 poliovirus VP1 protein is attenuating. J. Virol. **66:**3194–3197.
29. **Tracy, S., N. M. Chapman, J. Romero, and A. I. Ramsingh.** 1996. Genetics of coxsackievirus B cardiovirulence and inflammatory heart muscle disease. Trends Microbiol. **4:**175–179.
30. **Tu, A., N. M. Chapman, G. Hufnagel, S. Tracy, J. Romero, W. H. Barry, L. Zhao, K. Currey, and B. Shapiro.** 1995. The cardiovirulent phenotype of coxsackievirus B3 is determined at a single site in the genomic 5′ nontranslated region. J. Virol. **69:**4607–4618.
31. **Westrop, G. D., K. A. Wareham, D. M. A. Evans, G. Dunn, P. D. Minor, D. I. Magrath, F. Taffs, S. Marsden, M. A. Skinner, G. C. Schild, and J. W. Almond.** 1989. Genetic basis of attenuation of the Sabin type 3 oral poliovirus vaccine. J. Virol. **63:**1338–1344.
32. **Wiegers, K., H. Uhlig, and R. Dernick.** 1989. NAg1B of poliovirus type 1: a discontinuous epitope formed by two loops of VP1 comprising residues 96–104 and 141–152. Virology **170:**583–586.
33. **Willemer, S., and G. Adler.** 1989. Histochemical and ultrastructural characteristics of tubular complexes in human acute pancreatitis. Dig. Dis. Sci. **34:**46–55.
34. **Wolfgram, L. J., K. W. Beisel, and N. R. Rose.** 1985. Heart-specific autoantibodies following murine coxsackievirus B3 myocarditis. J. Exp. Med. **161:** 1112–1121.
35. **Zhang, H. Y., G. E. Yousef, L. Cunningham, N. W. Blake, X. OuYang, T. A. Bayston, R. Kandolf, and L. C. Archard.** 1993. Attenuation of a reactivated cardiovirulent coxsackievirus B3: the 5′-nontranslated region does not contain major attenuation determinants. J. Med. Virol. **41:**129–137.